Chemosphere 354 (2024) 141712

Contents lists available at ScienceDirect

Chemosphere

journal homepage: www.elsevier.com/locate/chemosphere

The actinomycete *Kitasatospora* sp. SeTe27, subjected to adaptive laboratory evolution (ALE) in the presence of selenite, varies its cellular morphology, redox stability, and tolerance to the toxic oxyanion

Andrea Firrincieli [a,1], Enrico Tornatore [b,1], Elena Piacenza [b], Martina Cappelletti [c], Filippo Saiano [d], Francesco Carfì Pavia [e], Rosa Alduina [b], Davide Zannoni [c], Alessandro Presentato [b,*]

[a] Department for Innovation in Biological, Agro-Food and Forest Systems (DIBAF), University of Tuscia, Via San Camillo de Lellis snc, 01100, Viterbo, Italy
[b] Department of Biological, Chemical and Pharmaceutical Sciences and Technologies (STEBICEF), University of Palermo, Viale delle Scienze Ed. 16, 90128, Palermo, Italy
[c] Department of Pharmacy and Biotechnology (FABIT), University of Bologna, Via Irnerio 42, 40126, Bologna, Italy
[d] Department of Agricultural, Food and Forestry Sciences (SAAF), University of Palermo, Viale delle Scienze Ed. 4, 90128, Palermo, Italy
[e] Department of Engineering, University of Palermo, Viale delle Scienze Ed. 8, 90128, Palermo, Italy

HIGHLIGHTS

- The rare actinomycete *Kitasatospora* sp. SeTe27 strain is notably tolerant to selenite.
- Adaptive Laboratory Evolution (ALE) enhances selenite microbial resistance.
- The ALE variant shows increased selenite uptake and redox stability.
- The ALE strain acquires missense mutations on antibiotic-related genes.
- Attenuation of metabolic processes favors bacterial survival under selenite pressure.

GRAPHICAL ABSTRACT

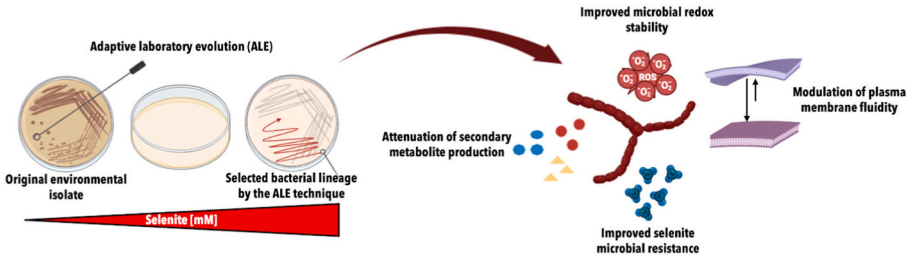

ARTICLE INFO

Keywords:
Selenite
Kitasatospora
Actinomycete
Oxidative stress
Whole-genome sequencing
Adaptive laboratory evolution

ABSTRACT

The effects of oxyanions selenite (SeO_3^{2-}) in soils are of high concern in ecotoxicology and microbiology as they can react with mineral particles and microorganisms. This study investigated the evolution of the actinomycete *Kitasatospora* sp. SeTe27 in response to selenite. To this aim, we used the Adaptive Laboratory Evolution (ALE) technique, an experimental approach that mimics natural evolution and enhances microbial fitness for specific growth conditions. The original strain (wild type; WT) isolated from uncontaminated soil gave us a unique model system as it has never encountered the oxidative damage generated by the prooxidant nature of selenite. The WT strain exhibited a good basal level of selenite tolerance, although its growth and oxyanion removal capacity were limited compared to other environmental isolates. Based on these premises, the WT and the ALE strains, the latter isolated at the end of the laboratory evolution procedure, were compared. While both bacterial strains had similar fatty acid profiles, only WT cells exhibited hyphae aggregation and extensively produced membrane-like

* Corresponding author.
E-mail addresses: andrea.firrincieli@unitus.it (A. Firrincieli), enrico.tornatore@unipa.it (E. Tornatore), elena.piacenza@unipa.it (E. Piacenza), martina.cappelletti2@unibo.it (M. Cappelletti), filippo.saiano@unipa.it (F. Saiano), francesco.carfipavia@unipa.it (F.C. Pavia), rosa.alduina@unipa.it (R. Alduina), davide.zannoni@unibo.it (D. Zannoni), alessandro.presentato@unipa.it (A. Presentato).
[1] Equally contributed.

https://doi.org/10.1016/j.chemosphere.2024.141712
Received 3 January 2024; Received in revised form 21 February 2024; Accepted 12 March 2024
Available online 12 March 2024

vesicles when grown in the presence of selenite (challenged conditions). Conversely, ALE selenite-grown cells showed morphological adaptation responses similar to the WT strain under unchallenged conditions, demonstrating the ALE strain improved resilience against selenite toxicity. Whole-genome sequencing revealed specific missense mutations in genes associated with anion transport and primary and secondary metabolisms in the ALE variant. These results were interpreted to show that some energy-demanding processes are attenuated in the ALE strain, prioritizing selenite bioprocessing to guarantee cell survival in the presence of selenite. The present study indicates some crucial points for adapting *Kitasatospora* sp. SeTe27 to selenite oxidative stress to best deal with selenium pollution. Moreover, the importance of exploring non-conventional bacterial genera, like *Kitasatospora*, for biotechnological applications is emphasized.

1. Introduction

Selenium (Se) is a crucial micronutrient for the health of living organisms (Genchi et al., 2023). Contrarily to essential metals such as copper, zinc, and manganese, selenium does not behave as an enzymatic cofactor since it is involved, as selenocysteine, in the active site of important selenoproteins, such as glutathione peroxidases, thioredoxin reductases, and iodothyronine deiodinases (Zoidis et al., 2018). These selenoproteins regulate various biological functions, including antioxidant defense, hormone balance, immune system support, and DNA repair (Genchi et al., 2023). However, selenium can be toxic at concentrations higher than the human diet requirement. The toxicity of selenium depends on its speciation (Fordyce, 2013), as Se exists in different valence states, including oxyanions selenate (SeO_4^{2-}, +6), and selenite (SeO_3^{2-}, +4), elemental selenium (0), and organoselenides (−2). Oxyanions are the most toxic due to their solubility and bioavailability, being selenite more toxic than selenate for most organisms (Ečimović et al., 2018). Conversely, elemental selenium (Se^0; insoluble) and selenides (e.g., H_2Se; volatile) have limited bioavailability, which reduces their potential harm to environmental safety and public health (Cappelletti et al., 2021).

The mechanisms underlying the toxicity of metal(loid) oxyanions, such as selenite or tellurite, are not yet fully understood. Nevertheless, research established that selenite induces oxidative stress by interacting with molecules containing thiol (SH) groups within cells, increasing the reactive oxygen species (ROS) level and causing oxidative damage (Kessi et al., 2022). Moreover, cysteine substitution with selenocysteine in the polypeptide chain can alter the structure of proteins, leading to their malfunctioning (Zoidis et al., 2018). Regardless, microbial species can assimilate selenite to synthesize seleno-amino acids (Turner et al., 1998) or engage in dissimilative reactions leading to Se^0. Indeed, under anaerobic conditions, microbes utilize enzymes such as sulfite, fumarate, arsenate, and nitrate reductases, for which selenite is the terminal electron acceptor (Staicu and Barton, 2021). During oxic microbial growth, enzymes such as thioredoxin, chromate/selenite, glutathione, and sulfite reductases facilitate selenite reduction as a detoxification mechanism (Huang et al., 2021; Hunter, 2014; Wang et al., 2019; Xia et al., 2018). Microorganisms can also employ non-enzymatic reducing molecules like glutathione, hydrogen sulfide, and siderophores to transform selenite into its zero-valence state (Nancharaiah and Lens, 2015). Finally, microbes can attenuate selenite toxicity through volatilization – i.e., the addition of methyl groups to oxyanions – and biosorption, where bacterial cells adsorb oxyanions through interaction with surface-charged moieties (Eswayah et al., 2017; Kagami et al., 2013; Yu et al., 2018). These findings underscore how microorganisms adapt and respond to selenite stress using diverse strategies. This research is gaining momentum thanks to biotic selenite transformation's potential for remediation of polluted environments and the production of biogenic selenium nanoparticles and quantum dots, with significant biotechnological applications (Ojeda et al., 2020).

To date, most studies on metal(loid) bioprocessing focus on microorganisms isolated from selenite-polluted environments; yet, expanding this research on bacterial strains ubiquitous among ecological niches, even considering those that never experience the oxyanion stress, is significant to ensure the implementation of such approaches worldwide. Also, fine-tuning these processes relies on addressing and recognizing the mechanisms of bacterial tolerance, adaptation, response, and resistance toward selenite. Among bacterial strains relevant to biotechnology, those belonging to the Actinobacterial phylum constitute an ensemble of resourceful microorganisms due to their varied genetic and metabolic repertoire (Solecka et al., 2012). Specifically, the *Streptomycetaceae* family includes *Streptomyces*, *Streptacidiphilus*, and *Kitasatospora* bacterial genera (Kämpfer et al., 2014). The genus *Streptomyces* is relevant due to the ability of the belonging bacterial strains to synthesize many secondary active metabolites (Alam et al., 2022), alongside their proficiency in handling metal(loid) toxicity (Presentato et al., 2020). As a sister genus, the *Kitasatospora* one is far less explored since it belongs to the list of rare actinobacteria genera, i.e., non-*Streptomyces* strains whose isolation frequency is lower than that of *Streptomyces* ones using conventional methods (Tiwari and Gupta, 2013). Although at least 50 bioactive compounds have been discovered from *Kitasatospora* strains (Takahashi, 2017), very little information is available regarding their metal(loid) processing potential. The currently available literature reports solely on *Kitasatospora* strains isolated from soil contaminated with heavy metals. An early report describes the constitutive resistance of the *Kitasatospora cystarginea* NR-4 strain to nickel (Van Nostrand et al., 2007); a more recent work reports on the multiple heavy metal resistance of a *Kitasatospora* strain, linking this bacterial resistance to secondary metabolite production (Yun et al., 2020). Instead, scientific knowledge regarding the interaction and processing of metal(loid) oxyanions by *Kitasatospora* strains is lacking.

Implementing biotechnological strategies can rely on the genetic manipulation of a bacterial strain to improve its phenotype. However, recombinant DNA technology is not always straightforward to apply so to pursue a specific goal. The Adaptive Laboratory Evolution (ALE) technique, earlier reported by Novick and Szilard (1950), represents an experimental approach that emphasizes bacterial cell fitness to specific laboratory growth conditions (Sandberg et al., 2019), emulating organism evolution through long-term cultivation, using selective pressure as a driving force. The latter encompasses the selection of an evolved bacterial species that harbors advantageous mutations and/or recombination into its chromosome responsible for (i) changes in the bacterial cell physiology, (ii) transcription and translation processes, and (iii) metabolites and metabolic fluxes (Hirasawa and Maeda, 2022). Combining this technique with whole-genome sequencing can help understand the link between the evolved phenotype and genotype. Further, this technique can facilitate the development of microbial cell factories for biotechnology approaches, as recently highlighted for the hyper-selenium tolerance trait evolved by *Saccharomyces cerevisiae* (Gong et al., 2023).

Thus, a comprehensive investigation into the potential of the *Kitasatospora* sp. SeTe27 strain to cope with selenite oxyanions is presented. The importance of this research stems from the strain's unique background, having never encountered selenite stress due to its origin in uncontaminated soil devoted to farming and agriculture by a Sicilian dairy product company. Specifically, this study examines the *Kitasatospora* strain's tolerance to selenite and the mechanisms by which selenite exerts its toxicity. In addition, the ALE technique and whole-genome

sequencing of both the wild-type (WT) and evolved (ALE) strains contributed to gaining insights into the microbial mechanisms of adaptation and response to the challenge posed by selenite stress.

2. Material and methods

2.1. Bacterial strains

The mesophilic *Kitasatospora* sp. SeTe27 strain was isolated from uncontaminated soil using starch-casein agar medium, which consisted of (g L^{-1}) starch (10), casein (0.3), potassium nitrate (KNO_3; 2), magnesium sulfate heptahydrate ($MgSO_4{\cdot}7H_2O$; 0.05), dipotassium hydrogen phosphate (K_2HPO_4; 2), sodium chloride (NaCl; 2), calcium carbonate ($CaCO_3$; 0.02), ferrous sulfate heptahydrate ($FeSO_4{\cdot}7H_2O$; 0.01), and bacteriological agar (15).

The ALE technique allowed the generation of a genotypic variant of the original environmental isolate. To this aim, the latter was cultivated on a solid R5 complex medium (Piacenza et al., 2022) for 72 h at 30 °C under static conditions. Afterward, a single bacterial colony was sub-cultivated onto the R5 medium amended with 0.5 mM sodium selenite (Na_2SeO_3) as a selective pressure. This sub-cultivation process was reiterated four times, each lasting one week. Therefore, bacterial cells experience a given selenite concentration for one month before sub-culturing them with the next one. Over time, selenite concentrations were gradually increased (i.e., 0.5, 1, 1.5, 2, 3, 4, and 5 mM). The entire bacterial adaptation process lasted seven months.

For clarity, the original bacterial strain is designated as wild-type (WT) and the adapted one as ALE.

All the reagents were purchased from Merck Life Science S.r.l. (Milan, Italy), except where specified otherwise in the following sections.

2.2. Bacterial tolerance toward selenite oxyanions

Mycelium's synchronization, through nutrient starvation, was achieved by pre-growing the WT bacterial strain for 72 h at 30 °C with shaking at 180 rpm. This process was carried out in 50 mL of R5 medium, using 250 mL baffled flasks. Bacterial cells were then inoculated (1% v/v) in a fresh R5 medium supplemented with increasing concentrations of oxyanions, ranging from 0 to 100 mM. Cells were allowed to grow for 24 h before the biomass (1 mL) was harvested through centrifugation at 8000×*g* for 10 min. The biomass was washed three times with a saline solution containing 0.9% w/v NaCl to remove traces of selenite and culture broth. Finally, washed cells (20 μl) were seeded onto R5 agar plates and incubated at 30 °C under static conditions to allow bacterial colony growth.

2.3. Bacterial growth profile

Pre-cultivated WT or ALE strains were inoculated (1% v/v) in 50 mL of the R5 medium. Bacterial cultures were grown for 168 h in the absence or presence of 2 mM selenite. Every 24 h, aliquots (500 μL) of bacterial cultures were collected and centrifuged (8000×*g* for 10 min) to isolate the total protein content (mg mL^{-1}) (Piacenza et al., 2022), whose average value (n = 5) with standard deviations (SD) describes the bacterial growth profile as a function of time. Similarly, samples were collected to estimate selenite consumption and thiol oxidation.

2.4. Selenite determination assays

The selenite concentration was evaluated as published elsewhere (Kessi et al., 1999). The reaction mixture consisted of hydrochloric acid (HCl; 0.1 M, 10 mL), EDTA (0.1 M, 0.5 mL), sodium fluoride (NaF; 0.1 M, 0.5 mL), disodium oxalate ($Na_2C_2O_4$; 0.1 M, 0.5 mL), 0.1% v/v of 2, 3-diaminonaphthalene in 0.1 M HCl (2.5 mL), and cell-free spent medium containing 50 nmol of selenite. After 40 min at 40 °C, the reaction mixture was cooled down at room temperature, and the selenium-2, 3-diaminonaphthalene complex was extracted in the dark by adding hexane (6 mL). The absorbance of the organic phase was read at 377 nm using 1-cm path-length glass cuvettes and the spectrophotometer SPECTROstar® Nano (BMG Labtech, Milan, Italy). The calibration curve relies on the absorbance of known selenite nanomoles (i.e., 10, 20, 30, 40, 50, 100, and 150; $R^2 = 0.9952$). Data indicate the average value (n = 5) of the residual selenite concentration with SD as a function of time.

To determine selenite uptake, exponentially grown (24 h) *Kitasatospora* WT or ALE cells were exposed to two mM selenite for 6 h. Afterward, the cell-free spent medium, processed as described earlier, was assayed to estimate the residual selenite content, either in the absence or presence of 50 μM of the protonophore and electron-transfer uncoupler carbonyl-cyanide m-chlorophenylhydrazone (CCCP). Data indicate the average values (n = 3) of selenite μmols taken up by WT or ALE cells normalized for the total protein content with SD.

2.5. Reactive oxygen species (ROS) determination

Exponentially grown WT or ALE cells were harvested and washed three times with phosphate buffer saline (PBS) composed of (g L^{-1}) NaCl (8), potassium chloride (KCl; 0.2), disodium hydrogen phosphate (Na_2HPO_4; 1.44), and potassium dihydrogen phosphate (KH_2PO_4; 0.24) pH 7.4. Diluted cells (1:3 vol ratio) were incubated with increasing concentrations (0.5, 1, and 2 mM) of selenite and 50 μM of the ROS-sensitive probe dichlorofluorescein diacetate (DCF) in a multitier 96-well plate for 2 h at 30 °C with shacking (180 rpm). DCF fluorescence was collected at 525 nm upon excitation at 488 nm every 10 min using a multi-plate reader (Synergy HT Biotek). At the initial and final time points, bacterial cell aliquots (200 μL) served to estimate the total protein content to normalize DCF fluorescence emission. The latter is also corrected for DCF fluorescence emission in PBS only. Unchallenged cells were used to evaluate the physiological level of ROS produced over the considered timeframe. Data indicate the average value (n = 3) of DCF fluorescence emission (Intensity Counts g $protein^{-1}$) with SD as described elsewhere (Piacenza et al., 2022).

2.6. Thiol (RSH) oxidation assay

The oxidation of the intracellular RSH pool was evaluated as published elsewhere (Turner et al., 1999). Bacterial culture aliquots (1 mL) were sampled every 24 h up to 168 h either in the absence or presence of 2 mM selenite. Bacterial cell pellets were harvested by centrifugation (8000×*g* for 10 min) and suspended in 1 mL of lysis solution containing SDS (0.1% v/v), EDTA (5 mM), Trizma base/HCl (50 mM) pH 8.0, and 5, 5′-dithiobis(2-nitrobenzoic acid) (DTNB; 0.1 mM). Thus, bacterial cells were incubated at 37 °C for 30 min, allowing cell lysis to occur. Afterward, RSHs containing supernatants were collected by centrifuging samples at 15,000×*g* for 10 min. The absorbance of supernatants was read at 412 nm using 1-cm path-length glass cuvettes and the spectrophotometer SPECTROstar® Nano (BMG Labtech, Milan, Italy). RSH concentrations were calculated using the molar extinction coefficient (1.36×10^4 M^{-1} cm^{-1}) of DTNB and normalized to total cell protein evaluated at different time points. The content of RSH (μmol g $protein^{-1}$) calculated at time 0 was subtracted by those estimated over the timeframe of the assay. Data indicate the average value (n = 3) of the loss of reduced RSHs from the original pool with SD.

2.7. Superoxide dismutase (SOD) activity assay

Kitasatospora sp. SeTe27 WT and ALE selenite-growing cells were harvested and processed to isolate the soluble protein fraction as described elsewhere (Piacenza et al., 2022). Specifically, bacterial cell pellets were washed and resuspended in an extraction buffer (EB) and ultimately lysed through 5 steps (30 s each interspersed by 30 s of pause on ice) of sonication performed at 15 W (Vibra-CellTM Sonics and

Materials Inc. Danbury, CT, USA). Proteins were recovered through centrifugation (8000×*g* for 15 min at 4 °C) and precipitated by adding 2 vol of ice-cold acetone for 1 h at −80 °C. Protein pellets were obtained by centrifugation (15,000×*g* for 20 min at 4 °C) and dried by speed vacuum (Eppendorf® 5301 concentrator; Milan, Italy). Protein samples were finally resuspended in EB and quantified by the Bradford assay. 5 μg of the soluble protein fraction was used to perform the SOD activity assay, according to the manufacturer protocol of the superoxide dismutase activity kit (Merck Life Science S.r.l., Milan, Italy). Data are reported as the average value (n = 4) of the SOD activity percentage (%) with SD.

2.8. Scanning electron microscopy imaging

WT and ALE hyphae grown, for 72 h at 30 °C, onto the solid R5 medium in the absence or presence of 2 mM selenite were harvested with a sterile loop, washed twice with saline solution, and fixed, at four degrees for approximately 16 h, with aqueous glutaraldehyde (2.5% v/v) solution. Glutaraldehyde residues were removed by washing bacterial biomass three times with a saline solution and then dehydrated through three washing steps (10 min each) with increasing concentrations (30, 40, 50, 60, 70, 80, 90, and 100%) of ice-cold ethanol. Finally, bacterial hyphae were loaded onto carbon-coated copper grids (300 mesh), dehydrated at room temperature, coated with gold (Sputtering Scancoat Six, Edwards) for 60 s in an argon atmosphere, and imaged using a FEG-SEM microscope (QUANTA 200F, FEI) with an accelerating voltage of 10 kV (Piacenza et al., 2022). WT and ALE exponentially grown hyphae under 2 mM selenite pressure, fixed and dehydrated as described above, were also imaged using FEG-SEM FEI versa 3D™ (Thermo Fisher Scientific Electron Microscopy Solutions) operating in scanning transmission mode (STEM). STEM was used to image biogenic selenium nanoparticles (SeNPs), which isolation from WT and ALE bacterial biomasses and average size diameter estimation were carried out as reported elsewhere (Piacenza et al., 2021, 2023). The elemental composition analysis of the extract containing selenium nanoparticles was performed utilizing a Zeiss Sigma VP and Oxford Instruments INCAx-act. This analysis involved a single-point selection assessment of the nanoparticles, which were air-dried onto Crystalline Silicon wafers (type N/Phos, size 100 mm, obtained from University WAFER) and mounted on Specimen Aluminum stubs (supplied by TED PELLA, INC.).

2.9. Antimicrobial activity of cell-free spent media

The capability of the *Kitasatospora* WT or ALE cell-free spent media to inhibit the growth – as surface adherent cells – of the Gram-positive bacterial strain *Staphylococcus aureus* ATCC 25923 cells was assessed by disk diffusion assay as reported elsewhere (Vitale et al., 2022). *S. aureus* strain pre-grown for approximately 16 h at 37 °C with shacking (180 rpm) in the Luria Bertani (LB) medium, composed of (g L^{-1}) NaCl (10), yeast extract (5), and tryptone (10), was seeded onto LB agar (15 g L^{-1}) plates with a microbial titer of 10^8 colony-forming units per milliliter of culture (CFU mL^{-1}). Bacterial confluent growth occurred at 37 °C for 24 h under static conditions. Before bacterial growth, sterile disks soaked with 20 μL of filter (0.2 μm) sterilized cell-free spent media collected every 24 h, deriving from unchallenged *Kitasatospora* WT or ALE cells in the R5 medium, were placed on top of the *S. aureus* cell layer. Data relate to inhibition halos (mm) of *S. aureus* growth with SD as a function of the cell-free spent medium's sampling time.

2.10. Fatty acid methyl ester analysis

Kitasatospora WT and ALE cells grown up to their late exponential growth phase in the presence or absence of 2 mM selenite were harvested (8000×*g* for 10 min) and washed thrice with sterile deionized water. Afterward, bacterial biomasses, suspended in water, were treated as reported elsewhere (Sasser, 1990) to extract fatty acids, prepare methyl ester derivatives, and perform gas-chromatography analysis. A gas chromatographic instrument (Agilent 6890), with a flame ionization detector (FID) and a mass selective (MS) detector (Agilent 5975c), was used with a Carbowax capillary column (50 m length, 0.32 mm internal diameter, and 0.25 μm film thickness from Supelco, Italy). Chromatographic conditions: injector in splitless mode at 250 °C, carrier gas, Helium, at 1 mL min^{-1} and an oven temperature program of a 6-min isotherm at 40 °C, a linear temperature increase of 4 °C min^{-1} to 230 °C, held for 5 min. The FID was 250 °C while MS scan conditions were: source temperature 230 °C, interface temperature 280 °C, and mass scan range 33–500 amu. Compound identification relied on the NIST05 library. The FAME profiles were described by comparisons of mass-spectra with high-quality materials and confirmed by comparisons of their retention indices (RI) with data in the available literature or co-injection of authentic standards (FAME, fatty acid methyl esters, and BAME, bacterial acid methyl esters, from Supelco, Italy). The relative percentage composition of fatty acids relied on the peak area normalization of the FID profile, considering equal to 1 the response factor for each component and performing three replicates for each sample. The internal standard was the methyl ester of nonadecanoic acid ($C_{19:0}$). The total of commonly identified compounds accounted for 97.0–99.6%.

2.11. Kitasatospora genome sequencing, assembly, functional annotation of biosynthetic gene clusters (BGCs), and identification of mutations in the ALE variant

Kitasatospora WT and ALE strains were sequenced in a paired-end mode (PE X 150 bp) to a final coverage of 144X with an Illumina NovaSeq. WT's sequencing reads were checked for the presence of sequencing adapters and assembled into contigs using the Unicycler v0.5.0 software. The stand-alone version of the NCBI Prokaryotic Genome Annotation Pipeline (PGAP) allowed annotating the resulting contigs (158). This Whole Genome Shotgun project has been deposited at DDBJ/ENA/GenBank under the accession JAXCLC000000000. The version described in this paper is version JAXCLC010000000.

As for the annotation of BGCs, the Genbank file generated through PGAP was uploaded into antiSMASH and analyzed with default parameters (Blin et al., 2023).

To identify mutations acquired by the *Kitasatospora* ALE variant, the raw sequencing reads of the latter were aligned against the WT strain genome using the snippy v4.6.0 software, being single-nucleotide polymorphisms (SNPs) and INDELs (i.e., insertion and deletions) called according to a minimum coverage of 20 and a minimum quality nucleotide score of 20. InterPro was used to identify whether the SNPs and INDELs fall within the coding sequences (CDSs) for structural or functional domains (Paysan-Lafosse et al., 2023). AlphaFold2 multimer mode was used through the COSMIC^2 cloud platform to predict the structural model of *Kitasatospora* SulP (PGAPTMP_006314) with default parameters (Jumper et al., 2021). The software ChimeraX v1.6.1 allowed the visualization of the SulP structure and the presence of hydrogen bonds in it (Pettersen et al., 2021). Structural analysis of missing contacts was performed using default parameters: van der Waals overlap ≥ −0.4 Å and pseudobonds radius 0.074 Å.

3. Results

3.1. Tolerance of Kitasatospora sp. SeTe27 strain to selenite oxyanions

The WT SeTe27 strain exhibited strong tolerance to selenite oxyanions (Fig. 1). There was no noticeable difference in the growth and development of the mycelium on solid media between cells exposed to selenite and the control cells at concentrations up to 10 mM oxyanions. As the selenite concentration increased (up to 20 mM), the natural brownish pigmentation of the mycelium gradually diminished. However, bacterial growth remained nearly confluent until reaching a concentration of 50 mM. It took much higher concentrations of selenite,

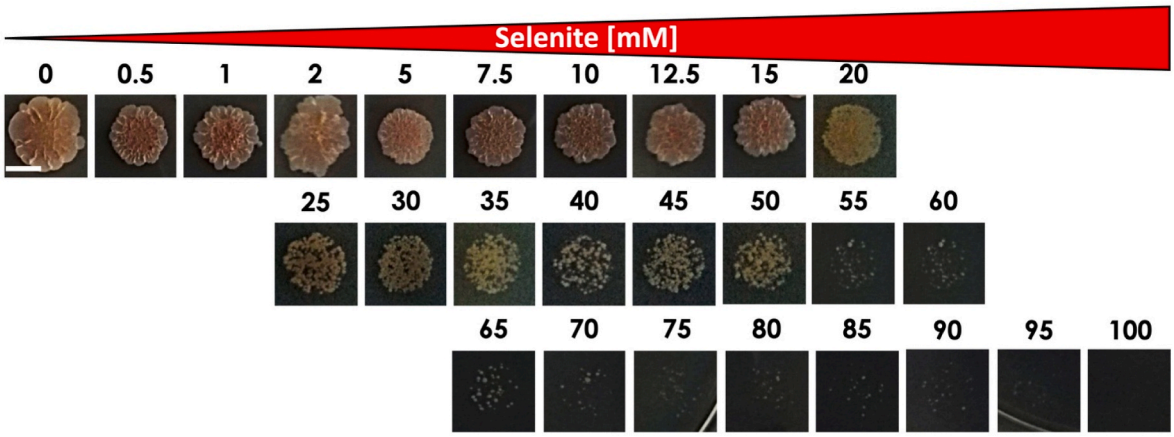

Fig. 1. *Kitasatospora* sp. SeTe27 WT tolerance toward selenite oxyanion: mycelium growth and development on solid media consequently to the challenge exerted by increasing selenite concentration (mM). The scale bar is 1 cm.

ranging from 55 to 95 mM, to significantly impair mycelium development, leading to the appearance of scattered colonies. Only at the highest selenite concentration tested (100 mM) did biomass growth inhibition occur, marking the minimal bactericidal concentration (MBC) of selenite for this *Kitasatospora* strain.

3.2. Growth profiles and selenite consumption capacities of Kitasatospora sp. SeTe27 WT and ALE strains

The growth profiles of SeTe27 WT and ALE strains (Fig. 2A) were studied in the presence of 2 mM selenite, whose concentration exceeds that found in various environmental settings (Sharma et al., 2009). Under selenite-free growth conditions, both WT and ALE strains exhibited similar growth trends, with a rapid growth phase lasting 48 h, following a stationary phase lasting up to 168 h. The protein content from 72 h onwards showed minor differences between the two strains, suggesting comparable survival capacities; however, upon selenite incubation, the WT strain exhibited a prolonged lag phase of at least 72 h before active growth occurred. The growth of the WT strain peaked between 96 and 120 h, subsequently reaching a stationary phase. Instead, the ALE variant displayed a shorter lag phase (24 h), indicating its evolved traits for a rapid adaptation to selenite stress. The growth profiles of the two strains reflected their ability to consume selenite over time (Fig. 2B). Initially, WT cells showed limited selenite consumption but gradually removed approximately 0.6 mM within 168 h. Differently, the ALE variant consumed 2 mM selenite within 72 h. Consistently, the ALE variant exhibited a higher uptake capacity (Table 1), being more than twice as high as that evaluated for the WT strain. Notably, the addition of 50 μM CCCP, a protonophore and electron-transport uncoupler, abolished the uptake of selenite oxyanions by both strains, suggesting that the oxyanion internalization depends on an electrochemical proton gradient (Borsetti et al., 2003).

Table 1
Selenite uptake performed by exponentially grown *Kitasatospora* sp. SeTe27 WT and ALE cells after 6 h of cell exposure to oxyanions.

	Selenite uptake (μmols g protein^{-1})	
Challenge	*Kitasatospora* WT	*Kitasatospora* ALE
Selenite	40.8 ± 7.6	105.6 ± 2.8
Selenite/CCCP	13.9 ± 5.6	9.3 ± 4.6

3.3. Cellular stress and oxidative responses of Kitasatospora sp. SeTe27 WT and ALE strains under selenite pressure

The extended latency phase (72 h) observed in *Kitasatospora* sp. SeTe27 WT cells growing under selenite pressure (Fig. 2A) indicated cell stress occurrence, likely resulting from the prooxidant nature of selenite. Consequently, increasing concentrations of selenite (0.5, 1, and 2 mM) were used to challenge exponentially grown WT cells in the presence of the ROS probe sensor DCF. WT cells were susceptible to selenite-induced oxidative damage, as they exhibited an oxidative burst in response to oxyanions (Fig. 3A), whose magnitude was directly proportional to the selenite initial concentration (Fig. S1A). In contrast, the low DCF fluorescence emission (Fig. 3B) indicated no oxidative damage in the case of ALE cells. Indeed, although the highest oxyanion concentration appeared to induce ROS species in ALE selenite-exposed cells (Fig. S1B), these results were not statistically different than those for selenite-free

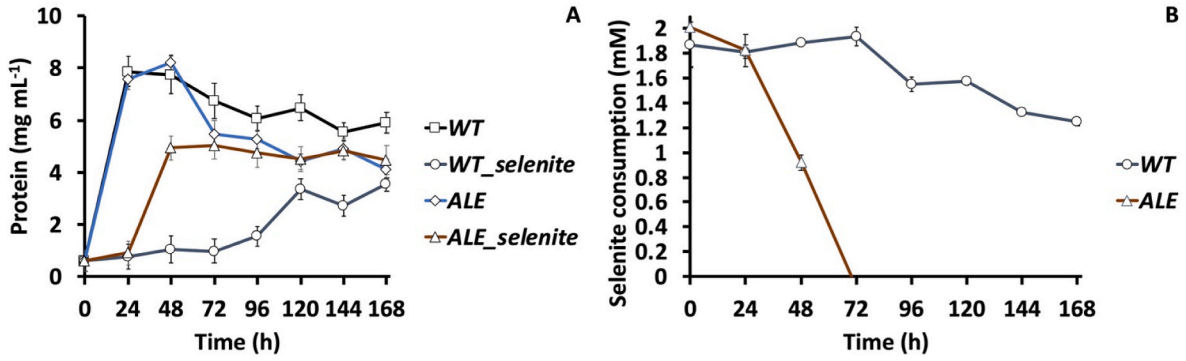

Fig. 2. *Kitasatospora* sp. SeTe27 WT and ALE strain cultures and residual selenite content determination: growth profiles in the absence or in the presence of 2 mM selenite (**A**) and selenite consumption kinetic (**B**).

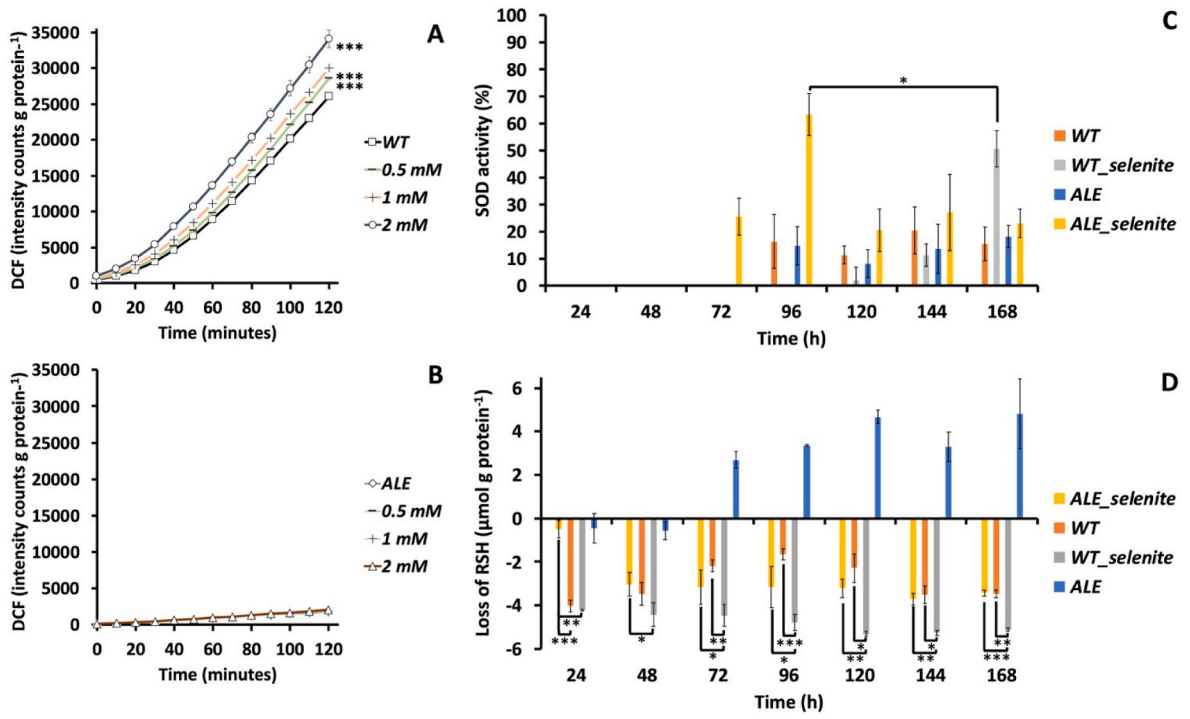

Fig. 3. ROS, SOD, and RSH content determination: kinetic of ROS production by the *Kitasatospora* sp. SeTe27 WT (**A**) and ALE (**B**) strains as a function of selenite concentration, SOD induction (**C**), and loss of the intracellular RSH pool (**D**) in the WT and ALE strains upon 2 mM selenite challenge over time (*p-value <0.05, **p-value <0.01, ***p-value <0.001).

ones, indicating the pronounced redox stability of the ALE strain compared to the WT one. This observation aligns with the evaluation of the intracellular reduced thiol (RSH) pool over the incubation time (Fig. 3D). Considering the level of RSH oxidation in the WT cells growing in the absence of selenite as physiological and dependent on the oxic growth condition, selenite-free ALE cells evidenced an adequate adaptation to the mere presence of oxygen, as highlighted by the building up of RSHs over time (Fig. 3D). In the case of the presence of selenite instead, WT cells accentuated the depletion of intracellular RSHs starting from 72 h onwards (end of the latency phase), thus suggesting the role of thiols as primary buffering molecules dealing with oxyanions. Contrarily, selenite-grown ALE cells featured a less oxidized intracellular environment than WT ones, with an extent of intracellular RSH loss comparable – except the 24-h timepoint that corresponds to the end of the lag phase – to that of selenite-free WT cells likely indicating that other biochemical systems than RSHs are involved in the biotic processing of oxyanions. Ultimately, both microorganisms activated superoxide dismutase (SOD) enzymes (Fig. 3C) to counteract the oxidative environment resulting from the downstream biotic conversion of selenite. Specifically, during the stationary phase (from 96 h onward), selenite-free growing WT and ALE cells induced this enzymatic activity, likely aiming to detoxify the cytosolic environment from byproducts of aerobic metabolism. Instead, SOD enzymes significantly increased in ALE and WT cells grown with selenite at 96 and 168 h, respectively. Indeed, these time points would correspond to incubation steps during which oxyanions might have already undergone reduction to their nontoxic elemental selenium form, consequently generating superoxide anions. Additionally, it is noteworthy that the ALE variant demonstrated a higher capacity for SOD production compared to the WT strain. This finding further supports the enhanced resilience of the evolved microbe when exposed to prooxidant oxyanions, effectively mitigating the potential occurrence of an oxidative burst.

3.4. Cell membrane adaptation and morphological changes in selenite-challenged Kitasatospora WT and ALE cells

Considering that the cell membrane represents the primary target of inorganic or organic stress incoming to bacterial cells, the fatty acids profile (Table 2) allowed us to evaluate how these microorganisms can respond to selenite. Regardless of the bacterial strains considered, bacterial cells decreased the amount of straight-chain fatty acids (SCFA), prioritizing the synthesis of branched ones (BFA). Among the latter, only those of the *iso* series increased in their relative percentage abundance, while the *anteiso*-$C_{15:0}$ fatty acid decreased. Most likely, this type of cell response allowed modulation of the plasma membrane fluidity, enabling bacterial cells to acclimatize to the presence of oxyanions.

From a morphological point of view, unchallenged WT hyphae exhibited a clean and smooth surface texture with some degree of cell

Table 2
Fatty acids profile of *Kitasatospora* sp. SeTe27 WT and ALE cells grew up to the late exponential growth phase in the absence or presence of selenite (2 mM).

Fatty acid	Relative abundance (%)			
	Kitasatospora WT		*Kitasatospora* ALE	
	Unchallenged	Selenite-challenged	Unchallenged	Selenite-challenged
$C_{14:0}$	2.59 ± 0.10	1.94 ± 0.01	3.45 ± 0.01	2.42 ± 0.13
$C_{15:0}$	3.61 ± 0.12	2.57 ± 0.03	4.14 ± 0.01	3.11 ± 0.15
$C_{16:0}$	41.3 ± 0.8	34.3 ± 0.1	50.7 ± 0.1	44.6 ± 0.1
$C_{17:0}$	0.77 ± 0.10	0.69 ± 0.01	1.05 ± 0.01	0.83 ± 0.08
$C_{18:0}$	1.02 ± 0.04	0.30 ± 0.01	0.98 ± 0.03	0.59 ± 0.08
[a]*iso*-$C_{15:0}$	23.83 ± 0.23	30.03 ± 0.23	8.29 ± 0.09	20.14 ± 0.11
[a]*anteiso*-$C_{15:0}$	13.5 ± 0.4	7.61 ± 0.25	21.5 ± 0.2	16.2 ± 0.7
[a]*iso*-$C_{16:0}$	5.30 ± 0.06	9.02 ± 0.01	4.08 ± 0.05	5.30 ± 0.22
[a]*iso*-$C_{17:0}$	6.63 ± 0.19	11.3 ± 0.1	2.99 ± 0.06	5.77 ± 0.08
$C_{16:1}$	1.46 ± 0.16	2.22 ± 0.02	2.84 ± 0.01	1.03 ± 0.07

[a] *Iso* and *anteiso* indicate the position of the methyl-substituent at the penultimate or antepenultimate carbon of the carboxyalkyl chain.

turgor and a few superficial membrane blebs emerging from the bacterial surface (Fig. 4A), whereas, unchallenged ALE hyphae exhibited characteristics of an aged mycelial stage (Fig. 4C), consistent with the strong adaptation of the ALE variant to the cultivation medium, leading to faster development and aging than the WT strain. Membrane blebs became more pronounced when WT hyphae were grown in the presence of selenite (Fig. 4B), suggesting a stress response aimed at regulating the homeostasis of selenite and its oxidation products. Besides, these hyphae appeared more swollen and aggregated to one another (Fig. 4B), indicating WT's tendency to reduce their surface area, potentially limiting oxyanion's entry into the bacterial cell cytosol. This observation aligns with the few exponentially selenite-grown WT hyphae showing an electron density attributable to the presence of selenium, either as oxyanion or in its elemental state (Figs. S2A and B). In selenite-grown ALE hyphae, these superficial blebs occurred with similar frequency to the unchallenged WT ones (Fig. 4D). Furthermore, the ALE hyphae featured a more intense and homogeneously distributed electron density under selenite pressure than WT ones (Figs. S2C and D), supporting the enhanced capability of the ALE variant in handling selenite toxicity and to biotically processes oxyanions. Nevertheless, both microorganisms could produce spherical selenium nanoparticles (SeNPs) as a product of selenite transformation (Figs. S3A and B), which, besides selenium, featured other elements (Fig. S 3C and D) attributable to the presence of a slight electron-dense material surrounding them. The difference between these biogenic nanomaterials regarded the average size diameter, as those generated by the WT strain were bigger (140 ± 40 nm) than those synthesized by the ALE variant (46 ± 13 nm).

3.5. Genomic insights into the selenite resistance trait of the Kitasatospora sp. SeTe27 ALE strain

Kitasatospora sp. SeTe27 WT genome was assembled into 158 contigs, accounting for an overall length of approximately 8.51 Mbp with a GC content of 73%. According to the PGAP, the WT strain possesses 7256 genes, among which 7056 are protein-coding genes (CDSs), 3 encodes for rRNA (i.e., 16S, 23S, and 5S), 70 for tRNA, 3 for non-coding RNA, and 133 pseudogenes. The ALE variant sequencing reads were aligned against the annotated genome of the WT strain to identify SNPs or INDELs possibly involved in the enhanced fitness of the former microorganism toward selenite. As a result, 38 SNPs, one deletion, and one complex variant were detected in the ALE strain genome (Table S1). Of these, 25 SNPs fall at the level of CDSs, and only 14 are missense mutations located in coding regions for catalytic or structural domains of transcription and translation factors, signal transduction proteins, transporters, and core genes of BGCs (Table 3). Some mutations may have had a notable effect on the fitness of the ALE strain when exposed to selenite oxyanions, influencing both primary and secondary metabolism and the strain's ability to uptake selenite. In particular, the structural prediction analysis of the sulfate permease (SulP) transporter (Fig. S4) indicates that this transporter is similar to the *Arabidopsis*

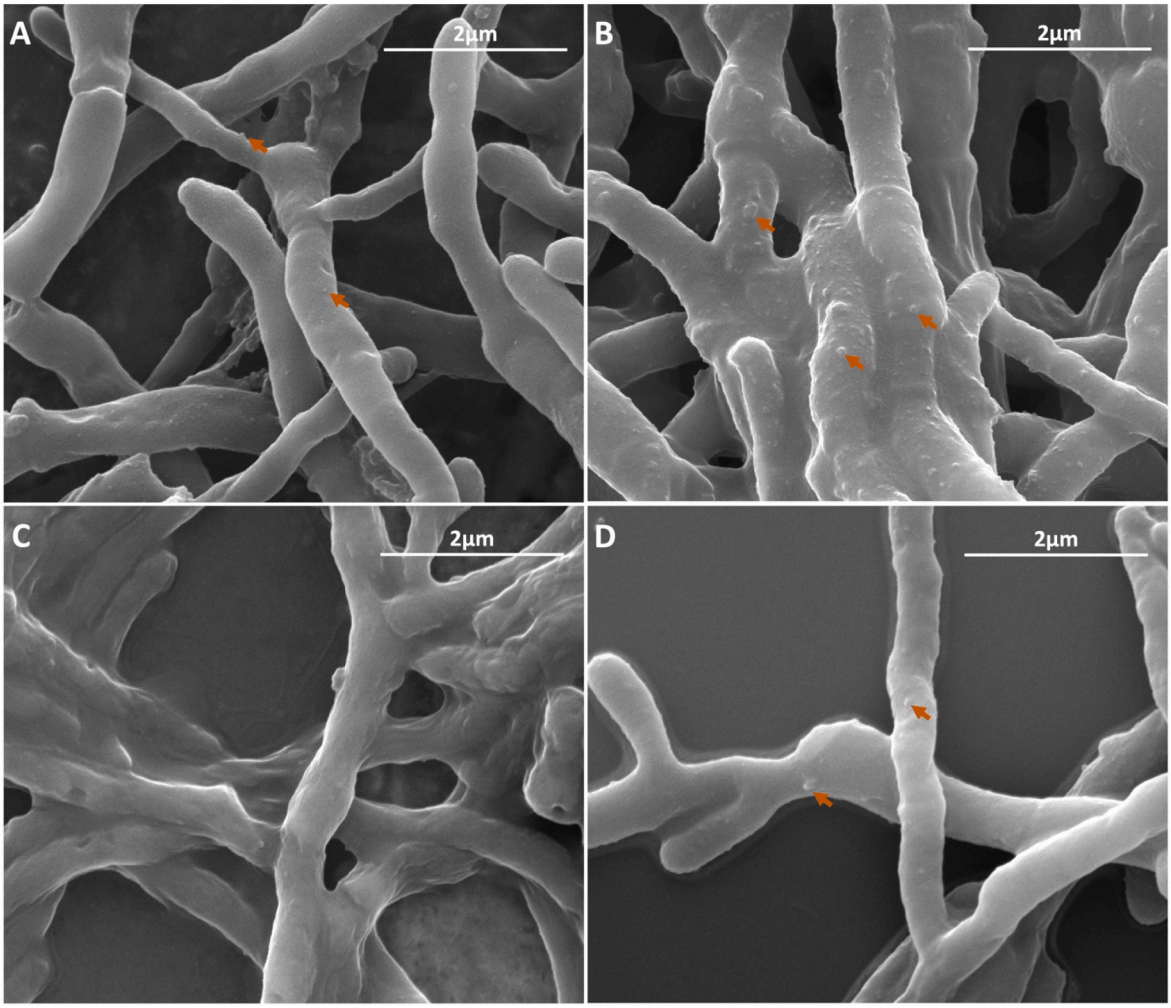

Fig. 4. *Kitasatospora* sp. SeTe27 hyphae's morphological features: unchallenged WT (**A**) and ALE (**B**) mycelium, while (**C**) and (**D**) depict those grown in the presence of 2 mM selenite. Arrows indicate surface membrane blebs.

Table 3
Missense mutations identified in the *Kitasatospora* sp. SeTe27 ALE strain genome.

Locus tag	Effect	Gene Product	Predicted function	Affected functional domain
001777	Ala6549Val	non-ribosomal peptide synthase/ polyketide synthase	Biosynthesis of secondary metabolites	13th condensation domain
004491	Asp731Ala	amino acid adenylation domain-containing protein		–
005291	Arg23Gly	response regulator transcription factor (DraR)		alpha-helix of the response regulator receiver domain
003756	Arg310Pro	DegT/DnrJ/ EryC1/StrS family aminotransferase	Unknown	–
004585	Val206Ile	pyridoxal-dependent decarboxylase	Metabolism of aromatic amino acids	Major domain
003444	Cys104Tyr	dipeptide ABC transporter ATP-binding protein	OppF, dipeptide uptake	ATP-binding domain
004215	Pro188Ala	TetR/AcrR family transcriptional regulator	LiuX, Isoleucine degradation	Repressor domain
004256	Leu204His	CbtA family protein	Cobalt uptake	5th TM alpha-helix
004455	Glu26Val	infB, translation initiation factor IF-2	protein synthesis	–
006314	Ala198Gly	SulP family inorganic anion transporter	anion:anion exchange transporter	7th TM alpha-helix
005760	Thr365Asn	ROK family transcriptional regulator	Unknown	–
006364	Arg17Trp	Ig-like domain-containing protein	Unknown	Signal peptide
007127	Glu9Ala	serine/threonine-protein kinase	Unknown	phosphorylase kinase domain 1
006013	Ser112Leu	hypothetical protein	Unknown	–

"-" indicates that the substitution does not fall in any of the functional/structural domains predicted via InterProScan.

thaliana sulfate:H^+ symporter AtSULTR4; 1 (Wang et al., 2021), featuring a C-terminal STAS domain, a gate domain consisting of transmembrane (TM) α-helices 5–7 and 12–14, and a core domain formed by TM α-helices 1–4 and 8–11, which carries the H^+/SO_4^{2-} symporter activity (Fig. S4A).

The ALE variant highlighted a substitution of alanine (Ala) at position 198 with glycine (Gly) located at the level of the TM α-helix 7 of the gate domain (Fig. S4B), which does not alter the backbone hydrogen bonds within this structural motif. However, this amino acidic substitution determines the loss of contact of glycine with leucine (Leu178) and tyrosine (Tyr174) residues of the TM α-helix 6, which could have influenced the oxyanion uptake (Table 1). Besides, the enhanced fitness of the ALE strain against selenite might be due to missense mutations targeting genes coding for proteins involved in the central carbon metabolism and the biosynthesis of secondary metabolites (Table 3). In this regard, the less proficiency of the ALE variant in producing antibiotic-like compounds capable of inhibiting the growth of the indicator pathogen *Staphylococcus aureus* ATCC 25923 strain than the WT one over time (Fig. 5) sustains this hypothesis.

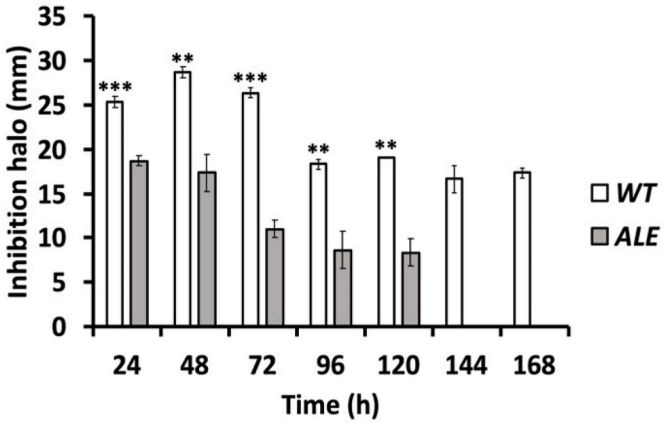

Fig. 5. Comparative antimicrobial efficacy of *Kitasatospora* WT and ALE strains against *Staphylococcus aureus* ATCC 25923: zone of inhibition halos (mm) estimated consequently to *S. aureus* cells growth in the presence of cell-free spent media collected, over the incubation, from the WT and ALE strain cultures (**p-value <0.01, ***p-value <0.001).

4. Discussion

4.1. *Kitasatospora sp. SeTe27 WT strain versus its ALE variant: the enhancement of selenite removal*

The realm of microorganisms encompasses many bacterial species able to simultaneously decontaminate selenite-polluted environments and recover selenium in a nontoxic and nanoscaled form via eco-friendly and sustainable processes rather than chemical-physical approaches (Ojeda et al., 2020). Nevertheless, studying bacterial strains that have never experienced the selenite challenge is paramount to understanding and acknowledging the microbial mechanisms for facing selenite toxicity, implementing existing biotechnological strategies, or developing new ones.

The rare actinomycete *Kitasatospora* sp. SeTe27 WT strain exhibited a notable tolerance towards selenite oxyanions (Fig. 1), aligning with that of other Gram-positive and -negative bacterial isolates under aerobic growth conditions (Amoozegar et al., 2008; Forootanfar et al., 2014; Khoei et al., 2017; Kiran Kumar Reddy et al., 2023; Presentato et al., 2018; Soudi et al., 2009; Zhang et al., 2019). This result gains significance since this environmental isolate has never encountered selenite in its natural habitat. Despite this good tolerance, the growth profile of the WT strain appears strongly impaired by selenite pressure (Fig. 2A), resulting in limited selenite removal (Fig. 2B), as opposed to other environmental isolates such as *Bacillus paramycoides* and *Bacillus mycoides* SelTE01 that completely removed more than 2 mM of selenite within 48-h (Baggio et al., 2021; Borah et al., 2021). To improve this trait in the SeTe27 strain, we applied the ALE technique to evolve a bacterial strain holding genotypic and, consequently, phenotypic advantages. Indeed, this technique successfully allowed obtaining evolved bacterial lineages featuring increased resistance to copper and arsenate ions, showcasing enhanced bioleaching efficiency and capacity (Ai et al., 2017; Maezato et al., 2012). The ALE variant exhibited a comparable outcome, as this evolved microbe now presents a shortened latency phase under selenite pressure (Fig. 2A). Additionally, it demonstrated more rapid kinetics of selenite removal (Fig. 2B) than the WT counterpart and similar to *Bacillus mycoides* SelTE01 and *Stenotrophomonas maltophilia* SelTE02, although these microbial isolates derived from the selenite hyperaccumulator legume *Astragalus bisulcatus* (Baggio et al., 2021; Lampis et al., 2014). As for the uptake of selenite oxyanions, the scientific literature indicates that this chemical species can utilize various transporters to enter the microbial cytosolic environment, such as low- and high-affinity phosphate transporters, the SmoK protein (i.e., an ABC-like transporter), the sulfate-thiosulfate (SulT) permease,

transporters for mono-carboxylates, and the aquaporin AqpZ (Aguilar-Barajas et al., 2011; Bébien et al., 2001; Lindblow-Kull et al., 1985; McDermott et al., 2010; Vriens et al., 2016; Xu et al., 2023; Zhu et al., 2020). Additional studies suggest that a proton motive force (PMF)-dependent transport is likely involved in selenite uptake since its entrance into the cell cytosol is partially inhibited by using protonophores dissipating the proton gradient (Xu et al., 2023). To date, the only solute:H^+ symporters that could be directly involved in the uptake of selenite are the lactate/pyruvate:H^+ symporter Jen1p (McDermott et al., 2010) and, given the structural similarity with sulfate, the sulfate:H^+ symporters SulP. Based on the PGAP, the SeTe27 strain possesses only one class of solute:H+ symporter potentially involved in the PMF-dependent selenite uptake, consisting of 5 copies of the *sulP* coding gene. Among these, three genes (locus tag 002533, 003762, and 006314) correlate to the ortholog group OG6_100144, which includes the functionally characterized sulfate transporters AtSULTR (i.e., 4; 1, 1; 1, and 1; 2) from *A. thaliana* and the sulfate transporter Rv1739c of *Mycobacterium tuberculosis* (Maruyama-Nakashita et al., 2004; Wang et al., 2021; Yamaguchi et al., 2017; Zolotarev et al., 2008). The remaining *sulP* coding genes (locus tag 000218 and 003827) correlate to ortholog groups that include the *Escherichia coli* DauA C4-dicarboxylic acid transporter (OG6_106724) and proteins with a carbonic anhydrase domain (OG6_100995), potentially involved in carbonic acid transport (Karinou et al., 2013). Considering that the protonophore action of CCCP abolished the selenite uptake (Table 1), as also reported elsewhere (Araie et al., 2011; McDermott et al., 2010), it is likely to conclude that an anion:H^+ symporter could be involved in selenite uptake in the SeTe27 strain. Interestingly, the ALE technique fixed a missense mutation in the gene 006314 coding for a SulP transporter (Fig. S4), causing the amino acidic substitution Ala198Gly in the TM α-helix 7 of the gate domain and, consequently, the loss of van der Waals interactions between the Ala-198 methyl-group and amino acidic residues of TM α-helix 6 (Fig. S4B). While Ala is not part of the central binding domain, the conformational changes occurring at the gate domain level control the access and release of the ligand in the cytosolic environment (Bavi et al., 2021). Thus, the loss of contacts between the TM α-helices 6 and 7 might influence the structural rearrangements of the gate domain (Bavi et al., 2021; Lindblow-Kull et al., 1985; Yu et al., 2017; Zolotarev et al., 2008), possibly explaining the improved selenite uptake capacity of the ALE variant (Table 1). In the latter strain, the adaptation to selenite pressure is shared and inherited by most of the hyphae, which synergistically participate in the oxyanion's active transportation within the cytosol (Figs. S2C and D). Conversely, in the WT strain, only a few hyphae seem involved in the oxyanion processing, as suggested by STEM images (Fig. S2 A and B). Further, the generation of bigger SeNPs by the WT strain than the ALE variant (Fig. S3) reflects this outcome. Indeed, when selenite enters only a few specialized WT hyphae, the local concentration of Se atoms within the cytoplasm generated through the oxyanion transformation will quickly reach the threshold concentration needed for SeNP formation, according to the LaMer mechanism (Thanh et al., 2014). Subsequently, other Se atoms available within the cytosol will adsorb onto the surface of the pre-formed SeNPs, causing their enlargement. In the ALE variant, the even distribution of selenite among hyphae likely determines a low concentration of Se atoms confined in the cell cytosol, thus allowing the growth of small NPs.

4.2. *Kitasatospora sp. SeTe27 evolving an enhanced redox stability*

One of the main microbial strategies counteracting selenite's toxicity relies on the oxyanion reduction into the less bioavailable and non-toxic Se^0 as either intracellular metal(loid) deposits or defined nanostructures (Presentato et al., 2020). RSH-containing molecules such as glutathiones (GHSs) and bacillithiols (BSHs) – typical of bacterial strains of the Proteobacteria and Firmicutes orders, respectively (Fahey, 2013) – are partially responsible for the biotic conversion of selenite, causing oxidative stress due to the formation of superoxide anions. Strictly aerobic microbes emphasize this phenomenon since they use oxygen as a terminal electron acceptor, thus exasperating the prooxidant nature of oxyanions (Tan et al., 2016). Actinomycetes mainly possess mycothiols (MSHs) that (i) feature enhanced redox stability compared to other RSH types, (ii) act as storage of cysteine, overcoming the auto-oxidation nature of the latter, and (iii) are less prone to auto-oxidation than GSHs (Newton et al., 2008). All these aspects reasonably explain the resistance and recovery of WT cells despite the oxidative burst evaluated upon selenite entry into the cell milieu (Fig. 3A). In line with this observation, selenite determined a decrease in RSHs in the WT strain than selenite-free cells (Fig. 3D), as also reported in the case of other microorganisms (Piacenza et al., 2021; Presentato et al., 2018; Tan et al., 2016; Zheng et al., 2014). Moreover, both WT and ALE strains showed a comparable loss of RSHs with their corresponding challenge within the latency phase, suggesting that RSHs either support the oxic bacterial growth (unchallenged growth condition) or are involved in the biotic conversion of selenite traces entering the cell cytosol (challenged growth condition). Overall, the ALE technique improved the redox stability and oxidative stress tolerance of the SeTe27 strain, likely due to the enhancement of MSH synthesis, as highlighted by the building up of the RSH content over time under unchallenging conditions of growth (Fig. 3D). In turn, the increased MSH availability in the ALE variant allowed a faster kinetic of selenite removal than the WT strain (Fig. 2B), indicating the occurrence of Painter-type reactions for the biotic conversion of oxyanions, which, however, did not correspond to the rising of ROS (Fig. 3B). This is due to the induction of genes coding for enzymes (i.e., superoxide dismutases) responsible for ROS detoxification (Kessi and Hanselmann, 2004); particularly, the ALE variant underscores how it has evolved an enhanced biochemical capacity inducing more SODs than the WT strain (Fig. 3C), thus allowing ALE cells for a fast bacterial recovery and prosper in a prooxidant environment compared to the WT counterpart, which is in agreement with earlier reports (Borsetti et al., 2005; Piacenza et al., 2022; Vrionis et al., 2015). Also, the ALE variant may induce genes coding for enzymes responsible for selenite bioconversion (Kessi et al., 2022). Thus, the ALE strain would accomplish a two-step action to deal with selenite, where one requires the involvement of a Painter-type reaction, while the other may rely on the induction of selenite-related enzymes (Piacenza et al., 2019). This bimodal action deployed by the ALE variant can allow a faster selenite uptake (Table 1) and biotic processing than the WT strain (Fig. 2B), reasonably explaining why the ALE cells can intensively uptake oxyanions within their exponential growth phase, remaining unaffected by the prooxidant stress deriving from this selenium chemical species. This aspect represents a step forward compared to other studies reporting on microbe-selenite interaction, where the actual uptake and bioconversion of oxyanions occur in the stationary phase of bacterial growth (Kessi et al., 2022), including microorganisms isolated from selenite-polluted environments.

4.3. *Cell membrane and morphology changes in response to selenite stress*

As for most xenobiotics, metal(loid) oxyanions primarily target the microbial cell membrane, causing severe perturbations and determining the impairment of several physiological functions (Konings et al., 2002). Bacteria can adapt and survive by maintaining their membrane integrity, for instance, modulating the type of fatty acids in response to whatever environmental stress bacterial cells are experiencing (Zhang and Rock, 2008). Specifically, Gram-positive bacterial strains mostly feature BFAs in their membrane (Kaneda, 1991), where *iso*-branched fatty acids tend to increase membrane rigidity compared to *anteiso* ones while responding to increased growth temperature, pH stress, or the presence of organic solvents that fluidize biological membranes (Giotis et al., 2007; Unell et al., 2007; Zhu et al., 2005). The effect of *iso*--branched fatty acid depends on its higher phase transition temperature than the *anteiso* form (Murínová and Dercová, 2014). Overall, the

selenite-growing *Kitasatospora* sp. SeTe27 WT and ALE cells increased the content of the *iso*-branched fatty acids (Table 2), which agrees with modifications observed in *Bacillus* sp. AR-6 and *Bacillus* sp. JS-2 strains experiencing high concentrations of selenite and the rare actinomycete *Micromonospora* sp. exposed to tellurite oxyanions (Dhanjal and Cameotra, 2011; Piacenza et al., 2022; Prakash et al., 2010) under aerobic conditions of growth. Thus, oxyanions may represent a trigger for bacterial cells to use branched-chain acyl-CoAs (i.e., methylbutyryl-CoA, isobutyryl-CoA, and isovaleryl-CoA) instead of acetyl-CoA or propionyl-CoA as a primer molecule to achieve BFA biosynthesis (Lu et al., 2004). In turn, this event constitutes an adaptive response leaning at improving the capacity of bacterial cells to repair potential membrane damages, strengthening its rigidity. Furthermore, the WT strain responded to selenite stress by undergoing hyphae aggregation (Fig. 4B), decreasing the cell surface area available and, in turn, mitigating the negative impact of such chemical species, as earlier observed for bacterial strains facing chromate, selenite, selenate, arsenate, or tellurite oxyanions (Antony et al., 2011; Chakravarty et al., 2007; Colin et al., 2013; Nepple and Bachofen, 1999; Piacenza et al., 2022). Another structural change observed was the enhanced formation of blebs emerging from selenite-grown WT hyphae's surface (Fig. 4B) compared to unchallenged or ALE ones (Fig. 4A and D). These structures resemble those produced by the *Micromonospora* sp. strain dealing with tellurite (Piacenza et al., 2022), thus reinforcing the hypothesis that, like streptomycetes (Schrempf et al., 2011), non-streptomycetes bacteria can exploit vesiculation phenomena to face environmental stresses. Unlike, the ALE strain highlighted such morphology changes (Fig. 4D) as frequently as unchallenged WT hyphae (Fig. 4A), further underlining its improved resilience trait toward selenite derived from the laboratory evolution process.

4.4. Primary and secondary metabolism link to selenite resistance in Kitasatospora sp. SeTe27 ALE variant: insights from missense mutations

The ALE variant displayed specific missense mutations predominantly in genes coding for products involved in both primary and secondary metabolism (Table 3), suggesting a potential link between these biological processes and the emergence of selenite resistance in the ALE strain. Notably, the DraR transcription factor (locus tag: 005291) of the DraR/DraK two-component system, as well as the transcription factor belonging to the ROK family, play a central role in controlling antibiotic biosynthesis, primary metabolism genes, morphological differentiation, carbon catabolite repression, and pH regulation in *S. coelicolor* (Burkovski et al., 2022; Świątek et al., 2013; Yu et al., 2014). The ALE technique also led to missense mutations in core genes of biosynthetic gene clusters that are directly involved in secondary metabolites biosynthesis. In particular, the ALE variant carried missense mutations falling in the 13th condensation domain of an NRP gene (locus tag 001777) located near the clifednamide biosynthetic gene cluster and in the coding sequence (locus tag 004491) for a protein containing an amino acid adenylation domain crucial for producing most secondary metabolites in microorganisms (Felnagle et al., 2008). These findings collectively indicate the reduction of the ALE variant's ability to synthesize secondary metabolites compared to the WT strain (Fig. 5). Thus, it is plausible that the selective pressure exerted by selenite on the ALE variant led to the attenuation of energy-demanding processes. This adaptation favored and prioritized selenite bioprocessing, a crucial challenge faced by the SeTe27 strain during the ALE procedure, serving as a defense mechanism aiming at counteracting selenite toxicity at the cellular level.

5. Conclusion

This study delves into the evolutionary dynamics of *Kitatasospora* sp. SeTe27 through the ALE technique to understand and improve microbial mechanisms for handling selenite toxicity. The findings present a multifaceted analysis of the ALE variant compared to the WT one, shedding light on diverse aspects such as selenite uptake and removal, redox stability, cell membrane adaptations, and genetic mutations.

The ALE technique significantly enhanced the SeTe27 strain selenite removal capacity, providing hints on the possible role of the SulP transporter, which, however, deserves further elucidation. Also, the ALE variant showcased improved redox stability and selenite bioprocessing capacity, outperforming its WT counterpart.

On a morphological level, the study highlights adaptive responses of the SeTe27 strain, including altered fatty acid composition, hyphae aggregation, and the formation of membrane-like vesicles, all aimed at mitigating the impact of selenite stress on the cell membrane. Moreover, the research identifies specific missense mutations in genes associated with primary and secondary metabolism in the ALE variant. These mutations potentially indicate a trade-off between energy-demanding processes and selenite bioprocessing, reflecting a defense mechanism prioritizing survival under selenite pressure.

In conclusion, this comprehensive study not only deepens our understanding of microbial adaptation to selenite toxicity but also underscores the potential of the ALE technique in enhancing microbial performances toward environmental stresses. The findings pave the way for future research, emphasizing the need for further exploration into the biochemical and genetic intricacies of microbial response to environmental stressors, thereby advancing our knowledge in biotechnology.

Funding sources

This work was funded by the European Union – NextGenerationEU – MUR D.M. funds. 737/2021 – research project granted to Alessandro Presentato.

CRediT authorship contribution statement

Andrea Firrincieli: Writing – review & editing, Investigation, Formal analysis, Data curation. **Enrico Tornatore:** Validation, Investigation. **Elena Piacenza:** Writing – review & editing, Formal analysis. **Martina Cappelletti:** Writing – review & editing, Resources. **Filippo Saiano:** Investigation, Data curation. **Francesco Carfì Pavia:** Investigation. **Rosa Alduina:** Writing – review & editing. **Davide Zannoni:** Writing – review & editing. **Alessandro Presentato:** Writing – original draft, Visualization, Supervision, Resources, Project administration, Funding acquisition, Formal analysis, Data curation, Conceptualization.

Declaration of competing interest

The authors declare that they have no known competing financial interests or personal relationships that could have appeared to influence the work reported in this paper.

Data availability

The genome version of the SeTe27 strain is available in FigShare (10.6084/m9.figshare.24885459). The Illumina reads of the ALE variant are available in SRA under the accession number SRR26946813.

Acknowledgments

The Ph.D. student Fanny Claire Capri (University of Palermo) is greatly acknowledged for the isolation of the *Kitasatospora* sp. SeTe27 strain. The Italian Ministry of Education, University, and Research and the REACT EU program is acknowledged to partially finance Andrea Firrincieli.

Appendix B. Supplementary data

Supplementary data to this article can be found online at https://doi.org/10.1016/j.chemosphere.2024.141712.

References

Aguilar-Barajas, E., Díaz-Pérez, C., Ramírez-Díaz, M.I., Riveros-Rosas, H., Cervantes, C., 2011. Bacterial transport of sulfate, molybdate, and related oxyanions. Biometals 24, 687–707. https://doi.org/10.1007/S10534-011-9421-X.

Ai, C., McCarthy, S., Liang, Y., Rudrappa, D., Qiu, G., Blum, P., 2017. Evolution of copper arsenate resistance for enhanced enargite bioleaching using the extreme thermoacidophile Metallosphaera sedula. J. Ind. Microbiol. Biotechnol. 44, 1613–1625. https://doi.org/10.1007/S10295-017-1973-5.

Alam, K., Mazumder, A., Sikdar, S., Zhao, Y.M., Hao, J., Song, C., Wang, Y., Sarkar, R., Islam, S., Zhang, Y., Li, A., 2022. *Streptomyces*: the biofactory of secondary metabolites. Front. Microbiol. 13, 968053 https://doi.org/10.3389/FMICB.2022.968053.

Amoozegar, M.A., Ashengroph, M., Malekzadeh, F., Reza Razavi, M., Naddaf, S., Kabiri, M., 2008. Isolation and initial characterization of the tellurite reducing moderately halophilic bacterium, *Salinicoccus* sp. strain QW6. Microbiol. Res. 163, 456–465. https://doi.org/10.1016/J.MICRES.2006.07.010.

Antony, R., Sujith, P.P., Sheryl Fernandes, S.O., Verma, P., Khedekar, V.D., Loka Bharathi, P.A., 2011. Cobalt immobilization by manganese oxidizing bacteria from the Indian ridge system. Curr. Microbiol. 62, 840–849. https://doi.org/10.1007/s00284-010-9784-1.

Araie, H., Sakamoto, K., Suzuki, I., Shiraiwa, Y., 2011. Characterization of the selenite uptake mechanism in the coccolithophore *Emiliania huxleyi* (Haptophyta). Plant Cell Physiol. 52, 1204–1210. https://doi.org/10.1093/PCP/PCR070.

Baggio, G., Groves, R.A., Chignola, R., Piacenza, E., Presentato, A., Lewis, I.A., Lampis, S., Vallini, G., Turner, R.J., 2021. Untargeted metabolomics investigation on selenite reduction to elemental selenium by *Bacillus mycoides* SeITE01. Front. Microbiol. 12 https://doi.org/10.3389/FMICB.2021.711000.

Bavi, N., Clark, M.D., Contreras, G.F., Shen, R., Reddy, B.G., Milewski, W., Perozo, E., 2021. The conformational cycle of prestin underlies outer-hair cell electromotility, 2021 Nature 600, 553–558. https://doi.org/10.1038/s41586-021-04152-4, 7889 600.

Bébien, M., Chauvin, J.P., Adriano, J.M., Grosse, S., Verméglio, A., 2001. Effect of selenite on growth and protein synthesis in the phototrophic bacterium *Rhodobacter sphaeroides*. Appl. Environ. Microbiol. 67, 4440–4447. https://doi.org/10.1128/AEM.67.10.4440-4447.2001.

Blin, K., Shaw, S., Augustijn, H.E., Reitz, Z.L., Biermann, F., Alanjary, M., Fetter, A., Terlouw, B.R., Metcalf, W.W., Helfrich, E.J.N., Van Wezel, G.P., Medema, M.H., Weber, T., 2023. antiSMASH 7.0: new and improved predictions for detection, regulation, chemical structures and visualisation. Nucleic Acids Res. 51 https://doi.org/10.1093/NAR/GKAD344. W46–W50.

Borah, S.N., Goswami, L., Sen, S., Sachan, D., Sarma, H., Montes, M., Peralta-Videa, J.R., Pakshirajan, K., Narayan, M., 2021. Selenite bioreduction and biosynthesis of selenium nanoparticles by *Bacillus paramycoides* SP3 isolated from coal mine overburden leachate. Environ. Pollut. 285, 117519 https://doi.org/10.1016/J.ENVPOL.2021.117519.

Borsetti, F., Toninello, A., Zannoni, D., 2003. Tellurite uptake by cells of the facultative phototroph *Rhodobacter capsulatus* is a ΔpH-dependent process. FEBS Lett. 554, 315–318. https://doi.org/10.1016/S0014-5793(03)01180-3.

Borsetti, F., Tremaroli, V., Michelacci, F., Borghese, R., Winterstein, C., Daldal, F., Zannoni, D., 2005. Tellurite effects on *Rhodobacter capsulatus* cell viability and superoxide dismutase activity under oxidative stress conditions. Res. Microbiol. 156, 807–813. https://doi.org/10.1016/j.resmic.2005.03.011.

Burkovski, A., Sprenger, G.A., Sánchez De La Nieta, R., Santamaría, R.I., Díaz, M., 2022. Two-component systems of *Streptomyces coelicolor*: an intricate network to be unraveled. Int. J. Mol. Sci. 23, 15085 https://doi.org/10.3390/IJMS232315085.

Cappelletti, M., Funari, V., Gasparotto, G., Dinelli, E., Zannoni, D., 2021. Selenium in the environment. In: Lens, P.N.L., Pakshirajan, K. (Eds.), Environmental Technologies to Treat Selenium Pollution: Principles and Engineering, pp. 101–130. https://doi.org/10.2166/9781789061055_0003.

Chakravarty, R., Manna, S., Ghosh, A.K., Banerjee, P.C., 2007. Morphological changes in an *Acidocella* strain in response to heavy metal stress. Res. J. Microbiol. 2, 742–748. https://scialert.net/abstract/?doi=jm.2007.742.748.

Colin, V.L., Villegas, L.B., Pereira, C.E., Amoroso, M.J., Abate, C.M., 2013. Morphological Changes and Oxidative Stress in Actinobacteria during Removal of Heavy Metals. CRC Press - Taylor & Francis Group. CRC Press, pp. 52–63. https://doi.org/10.1201/b14776.

Dhanjal, S., Cameotra, S.S., 2011. Selenite stress elicits physiological adaptations in *Bacillus* sp. (strain JS-2). J. Microbiol. Biotechnol. 21, 1184–1192. https://doi.org/10.4014/JMB.1105.05038.

Ečimović, S., Velki, M., Vuković, R., Štolfa Čamagajevac, I., Petek, A., Bošnjaković, R., Grgić, M., Engelmann, P., Bodó, K., Filipović-Marijić, V., Ivanković, D., Erk, M., Mijošek, T., Lončarić, Z., 2018. Acute toxicity of selenate and selenite and their impacts on oxidative status, efflux pump activity, cellular and genetic parameters in earthworm *Eisenia andrei*. Chemosphere 212, 307–318. https://doi.org/10.1016/J.CHEMOSPHERE.2018.08.095.

Eswayah, A.S., Smith, T.J., Scheinost, A.C., Hondow, N., Gardiner, P.H.E., 2017. Microbial transformations of selenite by methane-oxidizing bacteria. Appl. Microbiol. Biotechnol. 101, 6713. https://doi.org/10.1007/S00253-017-8380-8.

Fahey, R.C., 2013. Glutathione analogs in prokaryotes. Biochim. Biophys. Acta 5, 3182–3198. https://doi.org/10.1016/j.bbagen.2012.10.006.

Felnagle, E.A., Jackson, E.E., Chan, Y.A., Podevels, A.M., Berti, A.D., McMahon, M.D., Thomas, M.G., 2008. Nonribosomal peptide synthetases involved in the production of medically relevant natural products. Mol. Pharm. 5, 191–211. https://doi.org/10.1021/MP700137G.

Fordyce, F.M., 2013. Selenium deficiency and toxicity in the environment. In: Selinus, O. (Ed.), Essentials of Medical Geology: Revised Edition. Springer Netherlands, Springer Dordrecht, Heidelberg New York London, pp. 375–416. https://doi.org/10.1007/978-94-007-4375-5_16.

Forootanfar, H., Zare, B., Fasihi-Bam, H., Amirpour-Rostami, S., Ameria, A., Shakibaie, M., Nami, M.T., 2014. Biosynthesis and characterization of selenium nanoparticles produced by terrestrial actinomycete *Streptomyces microflavus* strain FSHJ31. Res Rev J Microbiol Biotechnol 3, 47–52.

Genchi, G., Lauria, G., Catalano, A., Sinicropi, M.S., Carocci, A., 2023. Biological activity of selenium and its impact on human health. Int. J. Mol. Sci. 24 https://doi.org/10.3390/ijms24032633.

Giotis, E.S., McDowell, D.A., Blair, I.S., Wilkinson, B.J., 2007. Role of branched-chain fatty acids in pH stress tolerance in *Listeria monocytogenes*. Appl. Environ. Microbiol. 73, 997–1001. https://doi.org/10.1128/AEM.00865-06.

Gong, A., Liu, W., Lin, Y., Huang, L., Xie, Z., 2023. Adaptive laboratory evolution reveals the selenium efflux process to improve selenium tolerance mediated by the membrane sulfite pump in *Saccharomyces cerevisiae*. Microbiol. Spectr. 11 https://doi.org/10.1128/spectrum.01326-23.

Hirasawa, T., Maeda, T., 2022. Adaptive laboratory evolution of microorganisms: methodology and application for bioproduction. Microorganisms 11, 92. https://doi.org/10.3390/MICROORGANISMS11010092.

Huang, S.W., Wang, Y., Tang, C., Jia, H.L., Wu, L., 2021. Speeding up selenite bioremediation using the highly selenite-tolerant strain *Providencia rettgeri* HF16-A novel mechanism of selenite reduction based on proteomic analysis. J. Hazard Mater. 406, 124690 https://doi.org/10.1016/J.JHAZMAT.2020.124690.

Hunter, W.J., 2014. *Pseudomonas seleniipraecipitans* proteins potentially involved in selenite reduction. Curr. Microbiol. 69, 69–74. https://doi.org/10.1007/S00284-014-0555-2.

Jumper, J., Evans, R., Pritzel, A., Green, T., Figurnov, M., Ronneberger, O., Tunyasuvunakool, K., Bates, R., Žídek, A., Potapenko, A., Bridgland, A., Meyer, C., Kohl, S.A.A., Ballard, A.J., Cowie, A., Romera-Paredes, B., Nikolov, S., Jain, R., Adler, J., Back, T., Petersen, S., Reiman, D., Clancy, E., Zielinski, M., Steinegger, M., Pacholska, M., Berghammer, T., Bodenstein, S., Silver, D., Vinyals, O., Senior, A.W., Kavukcuoglu, K., Kohli, P., Hassabis, D., 2021. Highly accurate protein structure prediction with AlphaFold. Nature 596, 583–589. https://doi.org/10.1038/s41586-021-03819-2.

Kagami, T., Narita, T., Kuroda, M., Notaguchi, E., Yamashita, M., Sei, K., Soda, S., Ike, M., 2013. Effective selenium volatilization under aerobic conditions and recovery from the aqueous phase by *Pseudomonas stutzeri* NT-I. Water Res. 47, 1361–1368. https://doi.org/10.1016/J.WATRES.2012.12.001.

Kämpfer, P., Glaeser, S.P., Parkes, L., Van Keulen, G., Dyson, P., 2014. The family *Streptomycetaceae*. In: Rosenberg, E., DeLong, E.F., Lory, S., Stackebrandt, E., Thompson, F. (Eds.), The Prokaryotes. Springer-Verlag Berlin Heidelberg, Springer, Berlin, Heidelberg, pp. 889–1010. https://doi.org/10.1007/978-3-642-30138-4_184.

Kaneda, T., 1991. Iso- and anteiso-fatty acids in bacteria: biosynthesis, function, and taxonomic significance. Microbiol. Rev. 55, 288–302. https://doi.org/10.1128/MR.55.2.288-302.1991.

Karinou, E., Compton, E.L.R., Morel, M., Javelle, A., 2013. The *Escherichia coli* SLC26 homologue YchM (DauA) is a C4-dicarboxylic acid transporter. Mol. Microbiol. 87, 623–640. https://doi.org/10.1111/MMI.12120.

Kessi, J., Hanselmann, K.W., 2004. Similarities between the abiotic reduction of selenite with glutathione and the dissimilatory reaction mediated by *Rhodospirillum rubrum* and *Escherichia coli*. J. Biol. Chem. 279, 50662–50669. https://doi.org/10.1074/jbc.M405887200.

Kessi, J., Ramuz, M., Wehrli, E., Spycher, M., Bachofen, R., 1999. Reduction of selenite and detoxification of elemental selenium by the phototrophic bacterium *Rhodospirillum rubrum*. Appl. Environ. Microbiol. 65, 4734–4740. https://doi.org/10.1128/AEM.65.11.4734-4740.1999.

Kessi, J., Turner, R.J., Zannoni, D., 2022. Tellurite and Selenite: how can these two oxyanions be chemically different yet so similar in the way they are transformed to their metal forms by bacteria? Biol. Res. 55, 1–25. https://doi.org/10.1186/s40659-022-00378-2.

Khoei, N.S., Lampis, S., Zonaro, E., Yrjälä, K., Bernardi, P., Vallini, G., 2017. Insights into selenite reduction and biogenesis of elemental selenium nanoparticles by two environmental isolates of *Burkholderia fungorum*. N. Biotech. 34, 1–11. https://doi.org/10.1016/J.NBT.2016.10.002.

Kiran Kumar Reddy, G., Pathak, S., Nancharaiah, Y.V., 2023. Aerobic reduction of selenite and tellurite to elemental selenium and tellurium nanostructures by *Alteromonas* sp. under saline conditions. Int. Biodeterior. Biodegrad. 179, 105571 https://doi.org/10.1016/J.IBIOD.2023.105571.

Konings, W.N., Albers, S.-V., Koning, S., Driessen, A.J.M., 2002. The cell membrane plays a crucial role in survival of bacteria and archaea in extreme environments. Antonie Leeuwenhoek 81, 61–72. https://doi.org/10.1023/A:1020573408652.

Lampis, S., Zonaro, E., Bertolini, C., Bernardi, P., Butler, C.S., Vallini, G., 2014. Delayed formation of zero-valent selenium nanoparticles by *Bacillus mycoides* SeiTE01 as a consequence of selenite reduction under aerobic conditions. Microb. Cell Factories 13, 1–14. https://doi.org/10.1186/1475-2859-13-35.

Lindblow-Kull, C., Kull, F.J., Shrift, A., 1985. Single transporter for sulfate, selenate, and selenite in *Escherichia coli* K-12. J. Bacteriol. 163, 1267. https://doi.org/10.1128/JB.163.3.1267-1269.1985.

Lu, Y.J., Zhang, Y.M., Rock, C.O., 2004. Product diversity and regulation of type II fatty acid synthases. Biochem. Cell. Biol. 82, 145–155. https://doi.org/10.1139/O03-076.

Maezato, Y., Johnson, T., McCarthy, S., Dana, K., Blum, P., 2012. Metal resistance and lithoautotrophy in the extreme thermoacidophile *Metallosphaera sedula*. J. Bacteriol. 194, 6856–6863. https://doi.org/10.1128/JB.01413-12.

Maruyama-Nakashita, A., Nakamura, Y., Watanabe-Takahashi, A., Yamaya, T., Takahashi, H., 2004. Induction of SULTR1;1 sulfate transporter in *Arabidopsis* roots involves protein phosphorylation/dephosphorylation circuit for transcriptional regulation. Plant Cell Physiol. 45, 340–345. https://doi.org/10.1093/PCP/PCH029.

McDermott, J.R., Rosen, B.P., Liu, Z., 2010. Jen1p: a high affinity selenite transporter in yeast. Mol. Biol. Cell 21, 3941. https://doi.org/10.1091/MBC.E10-06-0513.

Murínová, S., Dercová, K., 2014. Response mechanisms of bacterial degraders to environmental contaminants on the level of cell walls and cytoplasmic membrane. Internet J. Microbiol. 2014 https://doi.org/10.1155/2014/873081.

Nancharaiah, Y.V., Lens, P.N.L., 2015. Ecology and biotechnology of selenium-respiring bacteria. Microbiol. Mol. Biol. Rev. 79, 61–80. https://doi.org/10.1128/MMBR.00037-14.

Nepple, B.B., Bachofen, R., 1999. Morphological changes in phototrophic bacteria induced by metalloid oxyanions. Microbiol. Res. 154, 191–198. https://doi.org/10.1016/S0944-5013(99)80014-7.

Newton, G.L., Buchmeier, N., Fahey, R.C., 2008. Biosynthesis and functions of mycothiol, the unique protective thiol of actinobacteria. Microbiol. Mol. Biol. Rev. 72, 471–494. https://doi.org/10.1128/MMBR.00008-08.

Novick, A., Szilard, L., 1950. Experiments with the chemostat on spontaneous mutations of bacteria. In: Proceedings of the National Academy of Sciences of the United States of America. National Academy of Sciences, p. 708. https://doi.org/10.1073/PNAS.36.12.708.

Ojeda, J.J., Merroun, M.L., Tugarova, A.V., Lampis, S., Kamnev, A.A., Gardiner, P.H.E., 2020. Developments in the study and applications of bacterial transformations of selenium species. Crit. Rev. Biotechnol. 40, 1250–1264. https://doi.org/10.1080/07388551.2020.1811199.

Paysan-Lafosse, T., Blum, M., Chuguransky, S., Grego, T., Pinto, B.L., Salazar, G.A., Bileschi, M.L., Bork, P., Bridge, A., Colwell, L., Gough, J., Haft, D.H., Letunić, I., Marchler-Bauer, A., Mi, H., Natale, D.A., Orengo, C.A., Pandurangan, A.P., Rivoire, C., Sigrist, C.J.A., Sillitoe, I., Thanki, N., Thomas, P.D., Tosatto, S.C.E., Wu, C.H., Bateman, A., 2023. InterPro in 2022. Nucleic Acids Res. 51, D418–D427. https://doi.org/10.1093/NAR/GKAC993.

Pettersen, E.F., Goddard, T.D., Huang, C.C., Meng, E.C., Couch, G.S., Croll, T.I., Morris, J. H., Ferrin, T.E., 2021. UCSF ChimeraX: structure visualization for researchers, educators, and developers. Protein Sci. 30, 70–82. https://doi.org/10.1002/PRO.3943.

Piacenza, E., Campora, S., Carfì Pavia, F., Chillura Martino, D.F., Laudicina, V.A., Alduina, R., Turner, R.J., Zannoni, D., Presentato, A., 2022. Tolerance, adaptation, and cell response elicited by *Micromonospora* sp. facing tellurite toxicity: a biological and physical-chemical characterization. Int. J. Mol. Sci. 23, 12631. https://www.mdpi.com/1422-0067/23/20/12631.

Piacenza, E., Presentato, A., Bardelli, M., Lampis, S., Vallini, G., Turner, R.J., 2019. Influence of bacterial physiology on processing of selenite, biogenesis of nanomaterials and their thermodynamic stability. Molecules 24. https://doi.org/10.3390/MOLECULES24142532.

Piacenza, E., Presentato, A., Ferrante, F., Cavallaro, G., Alduina, R., Martino, D.F.C., 2021. Biogenic selenium nanoparticles: a fine characterization to unveil their thermodynamic stability. Nanomaterials 11, 1195. https://doi.org/10.3390/nano11051195.

Piacenza, E., Sule, K., Presentato, A., Wells, F., Turner, R.J., Prenner, E.J., 2023. Impact of biogenic and chemogenic selenium nanoparticles on model eukaryotic lipid membranes. Langmuir. https://doi.org/10.1021/ACS.LANGMUIR.3C00718.

Prakash, D., Pandey, J., Tiwary, B.N., Jain, R.K., 2010. Physiological adaptations and tolerance towards higher concentration of selenite (Se+4) in *Enterobacter* sp. AR-4, *Bacillus* sp. AR-6 and *Delftia tsuruhatensis* AR-7. Extremophiles 14, 261–272. https://doi.org/10.1007/S00792-010-0305-8.

Presentato, A., Piacenza, E., Anikovskiy, M., Cappelletti, M., Zannoni, D., Turner, R.J., 2018. Biosynthesis of selenium-nanoparticles and -nanorods as a product of selenite bioconversion by the aerobic bacterium *Rhodococcus aetherivorans* BCP1. N. Biotech. 41, 1–8. https://doi.org/10.1016/J.NBT.2017.11.002.

Presentato, A., Piacenza, E., Turner, R.J., Zannoni, D., Cappelletti, M., 2020. Processing of metals and metalloids by actinobacteria: cell resistance mechanisms and synthesis of metal(loid)-based nanostructures. Microorganisms 8, 2027. https://doi.org/10.3390/MICROORGANISMS8122027.

Sandberg, T.E., Salazar, M.J., Weng, L.L., Palsson, B.O., Feist, A.M., 2019. The emergence of adaptive laboratory evolution as an efficient tool for biological discovery and industrial biotechnology. Metab. Eng. 56, 1–16. https://doi.org/10.1016/J.YMBEN.2019.08.004.

Sasser, M., 1990. Bacterial identification by gas chromatographic analysis of fatty acids methyl esters (GC-FAME) [WWW Document]. URL. https://gcms.cz/labrulez-bucket-strapi-h3hsga3/paper/MIS_Technote_101.pdf, 8.30.23.

Schrempf, H., Koebsch, I., Walter, S., Engelhardt, H., Meschke, H., 2011. Extracellular *Streptomyces* vesicles: amphorae for survival and defence. Microb. Biotechnol. 4, 286–299. https://doi.org/10.1111/j.1751-7915.2011.00251.x.

Sharma, N., Prakash, R., Srivastava, A., Sadana, U.S., Acharya, R., Prakash, N.T., Reddy, A.V.R., 2009. Profile of selenium in soil and crops in seleniferous area of Punjab, India by neutron activation analysis. J. Radioanal. Nucl. Chem. 281, 59–62. https://doi.org/10.1007/s10967-009-0082-y.

Solecka, J., Zajko, J., Postek, M., Rajnisz, A., 2012. Biologically active secondary metabolites from actinomycetes. Cent. Eur. J. Biol. 7, 373–390. https://doi.org/10.2478/s11535-012-0036-1.

Soudi, M.R., Ghazvini, P.T.M., Khajeh, K., Gharavi, S., 2009. Bioprocessing of seleno-oxyanions and tellurite in a novel *Bacillus* sp. strain STG-83: a solution to removal of toxic oxyanions in presence of nitrate. J. Hazard Mater. 165, 71–77. https://doi.org/10.1016/J.JHAZMAT.2008.09.065.

Staicu, L.C., Barton, L.L., 2021. Selenium respiration in anaerobic bacteria: does energy generation pay off? J. Inorg. Biochem. 222, 111509 https://doi.org/10.1016/J.JINORGBIO.2021.111509.

Świątek, M.A., Gubbens, J., Bucca, G., Song, E., Yang, Y.H., Laing, E., Kim, B.G., Smith, C.P., Van Wezel, G.P., 2013. The ROK family regulator Rok7B7 pleiotropically affects xylose utilization, carbon catabolite repression, and antibiotic production in *Streptomyces coelicolor*. J. Bacteriol. 195, 1236–1248. https://doi.org/10.1128/JB.02191-12.

Takahashi, Y., 2017. Genus *Kitasatospora*, taxonomic features and diversity of secondary metabolites. J. Antibiot. (Tokyo) 70, 506–513. https://doi.org/10.1038/ja.2017.8.

Tan, Y., Yao, R., Wang, R., Wang, D., Wang, G., Zheng, S., 2016. Reduction of selenite to Se(0) nanoparticles by filamentous bacterium *Streptomyces* sp. ES2-5 isolated from a selenium mining soil. Microb. Cell Factories 15, 1–10. https://doi.org/10.1186/S12934-016-0554-Z.

Thanh, N.T.K., Maclean, N., Mahiddine, S., 2014. Mechanisms of nucleation and growth of nanoparticles in solution. Chem. Rev. 114, 7610–7630. https://doi.org/10.1021/CR400544S.

Tiwari, K., Gupta, R.K., 2013. Diversity and isolation of rare actinomycetes: an overview. Crit. Rev. Microbiol. 39, 256–294. https://doi.org/10.3109/1040841X.2012.709819.

Turner, R.J., Weiner, J.H., Taylor, D.E., 1999. Tellurite-mediated thiol oxidation in *Escherichia coli*. Microbiology (N. Y.) 145, 2549–2557. https://doi.org/10.1099/00221287-145-9-2549.

Turner, R.J., Weiner, J.H., Taylor, D.E., 1998. Selenium metabolism in *Escherichia coli*. Biometals 11, 223–227. https://doi.org/10.1023/A:1009290213301.

Unell, M., Kabelitz, N., Jansson, J.K., Heipieper, H.J., 2007. Adaptation of the psychrotroph *Arthrobacter chlorophenolicus* A6 to growth temperature and the presence of phenols by changes in the anteiso/iso ratio of branched fatty acids. FEMS Microbiol. Lett. 266, 138–143. https://doi.org/10.1111/j.1574-6968.2006.00502.x.

Van Nostrand, J.D., Khijniak, T.V., Gentry, T.J., Novak, M.T., Sowder, A.G., Zhou, J.Z., Bertsch, P.M., Morris, P.J., 2007. Isolation and characterization of four Gram-positive nickel-tolerant microorganisms from contaminated sediments. Microb. Ecol. 53, 670–682. https://doi.org/10.1007/S00248-006-9160-7.

Vitale, F., Saladino, M.L., Armetta, F., Presentato, A., Alduina, R., Mercadante, A., La Parola, V., Giacalone, F., 2022. New biocides based on imidazolinium-functionalised hybrid mesoporous silica nanoparticles. Microporous Mesoporous Mater. 343 https://doi.org/10.1016/J.MICROMESO.2022.112142.

Vriens, B., Behra, R., Voegelin, A., Zupanic, A., Winkel, L.H.E., 2016. Selenium uptake and methylation by the microalga *Chlamydomonas reinhardtii*. Environ. Sci. Technol. 50, 711–720. https://doi.org/10.1021/ACS.EST.5B04169.

Vrionis, H.A., Wang, S., Haslam, B., Turner, R.J., 2015. Selenite protection of tellurite toxicity toward *Escherichia coli*. Front. Mol. Biosci. 2, 69. https://doi.org/10.3389/fmolb.2015.00069.

Wang, D., Xia, X., Wu, S., Zheng, S., Wang, G., 2019. The essentialness of glutathione reductase GorA for biosynthesis of Se(0)-nanoparticles and GSH for CdSe quantum dot formation in *Pseudomonas stutzeri* TS44. J. Hazard Mater. 366, 301–310. https://doi.org/10.1016/J.JHAZMAT.2018.11.092.

Wang, L., Chen, K., Zhou, M., 2021. Structure and function of an *Arabidopsis thaliana* sulfate transporter. Nat. Commun. 12, 1–8. https://doi.org/10.1038/s41467-021-24778-2.

Xia, X., Wu, S., Li, N., Wang, D., Zheng, S., Wang, G., 2018. Novel bacterial selenite reductase CsrF responsible for Se(IV) and Cr(VI) reduction that produces nanoparticles in *Alishewanella* sp. WH16-1. J. Hazard Mater. 342, 499–509. https://doi.org/10.1016/J.JHAZMAT.2017.08.051.

Xu, Q., Zhang, S., Ren, J., Li, K., Li, J., Guo, Y., 2023. Uptake of selenite by *Rahnella aquatilis* HX2 involves the aquaporin AqpZ and Na+/H+ antiporter NhaA. Environ. Sci. Technol. 57, 2371–2379. https://doi.org/10.1021/ACS.EST.2C07028.

Yamaguchi, C., Ohkama-Ohtsu, N., Shinano, T., Maruyama-Nakashita, A., 2017. Plants prioritize phytochelatin synthesis during cadmium exposure even under reduced sulfate uptake caused by the disruption of SULTR1;2. Plant Signal. Behav. 12, e1325053 https://doi.org/10.1080/15592324.2017.1325053.

Yu, Q., Boyanov, M.I., Liu, J., Kemner, K.M., Fein, J.B., 2018. Adsorption of selenite onto *Bacillus subtilis*: the overlooked role of cell envelope sulfhydryl sites in the microbial conversion of Se(IV). Environ. Sci. Technol. 52, 10400–10407. https://doi.org/10.1021/ACS.EST.8B02280.

Yu, X., Yang, G., Yan, C., Baylon, J.L., Jiang, J., Fan, H., Lu, G., Hasegawa, K., Okumura, H., Wang, T., Tajkhorshid, E., Li, S., Yan, N., 2017. Dimeric structure of the uracil:proton symporter UraA provides mechanistic insights into the SLC4/23/26 transporters. Cell Res. 27, 1020–1033. https://doi.org/10.1038/cr.2017.83.

Yu, Z., Zhu, H., Zheng, G., Jiang, W., Lu, Y., 2014. A genome-wide transcriptomic analysis reveals diverse roles of the two-component system DraR-K in the physiological and morphological differentiation of *Streptomyces coelicolor*. Appl. Microbiol. Biotechnol. 98, 9351–9363. https://doi.org/10.1007/S00253-014-6102-Z.

Yun, B.R., Malik, A., Kim, S.B., 2020. Genome based characterization of *Kitasatospora* sp. MMS16-BH015, a multiple heavy metal resistant soil actinobacterium with high antimicrobial potential. Gene 733. https://doi.org/10.1016/J.GENE.2020.144379.

Zhang, J., Wang, Y., Shao, Z., Li, J., Zan, S., Zhou, S., Yang, R., 2019. Two selenium tolerant *Lysinibacillus* sp. strains are capable of reducing selenite to elemental Se

efficiently under aerobic conditions. J. Environ Sci. 77, 238–249. https://doi.org/10.1016/J.JES.2018.08.002.

Zhang, Y.M., Rock, C.O., 2008. Membrane lipid homeostasis in bacteria. Nat. Rev. Microbiol. 6, 222–233. https://doi.org/10.1038/nrmicro1839.

Zheng, S., Su, J., Wang, L., Yao, R., Wang, D., Deng, Y., Wang, R., Wang, G., Rensing, C., 2014. Selenite reduction by the obligate aerobic bacterium *Comamonas testosteroni* S44 isolated from a metal-contaminated soil. BMC Microbiol. 14, 1–14. https://doi.org/10.1186/S12866-014-0204-8.

Zhu, K., Bayles, D.O., Xiong, A., Jayaswal, R.K., Wilkinson, B.J., 2005. Precursor and temperature modulation of fatty acid composition and growth of *Listeria monocytogenes* cold-sensitive mutants with transposon-interrupted branched-chain α-keto acid dehydrogenase. Microbiology 151, 615–623. https://doi.org/10.1099/MIC.0.27634-0.

Zhu, T.T., Tian, L.J., Yu, H.Q., 2020. Phosphate-suppressed selenite biotransformation by *Escherichia coli*. Environ. Sci. Technol. 54, 10713–10721. https://doi.org/10.1021/ACS.EST.0C02175.

Zoidis, E., Seremelis, I., Kontopoulos, N., Danezis, G.P., 2018. Selenium-dependent antioxidant enzymes: actions and properties of selenoproteins. Antioxidants 7, 66. https://doi.org/10.3390/ANTIOX7050066.

Zolotarev, A.S., Unnikrishnan, M., Shmukler, B.E., Clark, J.S., Vandorpe, D.H., Grigorieff, N., Rubin, E.J., Alper, S.L., 2008. Increased sulfate uptake by *E. coli* overexpressing the SLC26-related SulP protein Rv1739c from *Mycobacterium tuberculosis*. Comp. Biochem. Physiol. Mol. Integr. Physiol. 149, 255–266. https://doi.org/10.1016/J.CBPA.2007.12.005.